IEEE Access
Multidisciplinary | Rapid Review | Open Access Journal

Received 25 December 2023, accepted 7 January 2024, date of publication 10 January 2024,
date of current version 18 January 2024.

Digital Object Identifier 10.1109/ACCESS.2024.3352129

RESEARCH ARTICLE

A Constrained Fuzzy Control for Robotic Systems

WENKUI XUE[1], BAOZHI ZHOU[1], FENGHUA CHEN[2], HAMID TAGHAVIFAR[3], (Member, IEEE), ARDASHIR MOHAMMADZADEH[4], AND EBRAHIM GHADERPOUR[5]

[1]School of Electrical Engineering, Changzhou Vocational Institute of Mechatronic Technology, Changzhou 213164, China
[2]School of Intelligent Manufacturing, Zhejiang Guangsha Vocational and Technical University of Construction, Dongyang 322100, China
[3]Department of Mechanical, Industrial and Aerospace Engineering, Concordia University, Montreal, QC H3G 1M8, Canada
[4]Multidisciplinary Center for Infrastructure Engineering, Shenyang University of Technology, Shenyang 110870, China
[5]Department of Earth Sciences, Sapienza University of Rome, 00185 Rome, Italy

Corresponding author: Ebrahim Ghaderpour (ebrahim.ghaderpour@uniroma1.it)

This work was supported in part by the Sapienza University of Rome.

ABSTRACT The use of wheeled mobile robots (MRs) with symmetrical structure in engineering is rapidly increasing, with applications in various fields, such as industry, agriculture, forestry, healthcare, mining, rehabilitation, search and rescue, household tasks, remote locations, and entertainment. As MRs become more common, researchers are focusing on developing better ways to model and control these robots to improve their performance and adaptability. The main challenges in this area include uncertain dynamics, non-holonomic constraints, and various perturbations, which complicate the design of the control system. This paper presents a new predictive control scheme for MRs that is independent of the dynamics and the robot's working environment. A Type-3 fuzzy logic system is developed to identify the MR dynamics online. The designed predictive scheme improves accuracy and speeds up convergence, while also addressing uncertainties and considering constraints on control input. Additionally, a chaotic-based system is proposed for secure path planning, generating a complex and unpredictable reference trajectory that is useful for patrol MR applications. The effectiveness of the suggested controller is demonstrated through simulations and experiments.

INDEX TERMS Fuzzy control, constrained control, type-3 fuzzy logic, mobile robot, chaotic systems.

NOMENCLATURE

MR	Mobile Robot.
SMC	Sliding-Mode Controller.
FLS	Fuzzy Logic System.
PI	Proportional-Integral.
MPC	Model-based Predictive Control.
T3	Type-3.
$d \in R$	Perturbation.
$\bar{H}_{\tilde{\Omega}_i^j \bar{\alpha}_i} / \bar{H}_{\tilde{\Omega}_i^j \underline{\alpha}_i}$	Upper memberships.
$\underline{H}_{\tilde{\Omega}_i^j \bar{\alpha}_i} / \underline{H}_{\tilde{\Omega}_i^j \underline{\alpha}_i}$	Lower memberships.
$\tilde{\Omega}_i^j$	j_{th} Membership function for i_{th} input.
$C_{\tilde{\Omega}_i^j}$	Center of $\tilde{\Omega}_i^j$.

The associate editor coordinating the review of this manuscript and approving it for publication was Yu-Da Lin.

I. INTRODUCTION

Mobile robots (MR) application in engineering systems is experiencing significant growth in recent years. This expansion spans a diverse range of sectors including industry, agriculture, forestry, mining, medicine, surgery, rehabilitation, healthcare, search and rescue, domestic use, operation in hazardous locations, remote area deployment, and entertainment. Wheeled MRs, which interact with surfaces through their wheels, exemplify these systems and are subject to non-holonomic constraints [33]. These constraints arise because the wheels are designed to roll forward without slipping, which limits their movement. Consequently, the motion control of wheeled MRs for automated operations presents several control challenges, including path following, stability, and maintaining a consistent trajectory [18], [19].

Due to the wide applications of MRs, the control problem of MRs has attracted great attention and many control methods have been developed. For example, in [5] sliding-mode controller (SMC) with gain adaptations for tracking

problem of MRs was investigated. The designed SMC compensated the external disturbances, and a kinematic controller was also applied to consider the non-holonomic constraints. In [29], first an integral backstepping controller was designed, and then to obtain the asymptotic convergence a recurve backstepping was developed. In [7], the wheeled MRs by non-holonomic constraints were studied, with a focus on analyzing the kinematic and SMC models.

An improved switching structure based on SMC was employed to control the robot's trajectory tracking, and the reduction of pose error and the accuracy of control of linear velocity and angular speed are studied. The fixed-time tracking control of MRs was studied in [24], and the fixed-time control laws are proposed based on Lyapunov analysis. Lyapunov's theory was also used in other studies to guarantee control system's stability, e.g., [8]. It was shown that the obtained settling time was independent to initial conditions, which makes it more practical. The formation control of MRs under non-holonomic restrictions was studied in [14]. The formation was converted into a consensus problem, and speed inputs are computed using continuously distributed protocols to decrease chattering. In [34], an adaptive SMC was designed, the actuator saturation is taken into account, and the asymptotic stability was studied.

In most classic controllers, such as the controllers mentioned above, MRs are taken into account and the controllers are constructed using mathematical models. FLSs have a wide applications in engineering, for example, explication of crossroads order [28], robot manipulators [15], determination of journeys order [26], control systems [4], and estimation problems [27]. To estimate the dynamics of MRs and identify the uncertain parameters and dynamics, some neuro-fuzzy controllers have been also developed. For example, in [17] the conventional SMC is combined with a Fuzzy Logic System (FLS), and it is shown that FLS is effective in the control of MRs.

A fuzzy proportional-integral (PI) control algorithm was proposed in [35] to analyze the omnidirectional movement of MRs. Experimental data verified that the fuzzy control algorithm notably diminished yaw error and enhances heading-regulation performance, outperforming traditional PI control algorithms. The motion model of spherical MRs was analyzed using FLSs in [12], and a fuzzy controller was designed accordingly. The response of a fuzzy controller was assessed in [1], and the computation time of an FLS-based controller was taken into account and a technique was developed to optimize the rules of FLS.

A comprehensive FLS-based control system, as proposed in [21], was developed for a two-wheeled balancing mobile robot (MR). This control system incorporated three distinct FLSs to manage position, balance, and directional control. The controllers within this system utilized optimally determined membership functions, which were refined through the cross-entropy optimization method. The effectiveness of the FLSs were demonstrated through real-time evaluation using an STM32F4 microcontroller.

Recently, type-3 FLSs have been suggested for the control and modeling of practical systems [22], [30]. For instance, in [3], the dynamics were estimated using T3-FLSs, and it was verified that T3-FLSs are more efficient in controlling Mobile Robots (MRs) in complex, uncertain environments. The path planning and following of MRs under practical perturbations were studied in [31], where a T3-FLS controller was suggested. Several experimental and simulation examinations demonstrated the superior response of T3-FLSs. In [6], besides the uncertain dynamics, the states of MRs were also considered unknown, leading to the design of a T3-FLS-based observer. A harmony search algorithm, utilizing T3-FLSs, was designed in [25] and was used for parameter estimation in a fuzzy control system for MRs. In [23], a fractional-order controller was developed using T3-FLSs, and new rules were suggested for the training of T3-FLSs based on stability analysis. Table 1 summarizes the studies carried out in this work.

The control algorithm utilized in the industry must possess specific features, such as being user-friendly and straightforward to adjust, as these serve as benchmarks for its widespread industrial application. Although traditional controllers are widely used in the industry, the varied behavior of industrial processes restricts their utility. This dynamic behavior is likely due to various factors, such as the existence of zeros outside the stable region, unstable poles, long and uncertain time-varying delays, and limitations on the process variables. The predictive control algorithm is a method designed to handle such complex processes, where the base path, known as the prediction horizon, is already established. The controller's output must now be determined so that the predicted output of the process aligns as closely as possible with the base path. Numerous methods falling under the umbrella of predictive control have been presented so far, leading to better, more accurate development and treatment. The most significant claim of this algorithm is its applicability to non-linear processes and its capability to maintain control [20]. Its ability to manage non-linear functions, which may vary over time, and under conditions with various restrictions on process variables, distinguishes these controllers as unique and superior compared to other methods. One of the effective controllers within this category is model-based predictive control (MPC).

The challenge with MPC is expressed as the need for a controller to bring the system's response to the desired value in the ensuing moment, using present-time information. The predictive controller possesses a system model capable of forecasting future behavior, known as a predictive model [2]. In fact, the basis of predictive controllers is as follows.

1) Forecasting model that determines future outputs for a forecast horizon based on past outputs and past and present inputs.
2) Predictive control whose purpose is to bring the output to a desired value in the future.

TABLE 1. A quick view on literature.

Reference	Method	Main contribution
[5]	SMC	Gain adaptations
[29]	Integral backstepping	Analyzing of asymptotic convergence
[7]	SMC	Studding the effect of non-holonomic constraints
[24]	Fixed-time tracking control	Fixed-time control laws based on Lyapunov analysis
[14]	Formation control	Studding the non-holonomic restrictions
[12]	Fuzzy control	Motion modeling
[34]	Adaptive SMC	Actuator saturation
[21]	Fuzzy control	Balancing of a two-wheeled mobile robot
[31]	Type-3 fuzzy control	Path planning
[23]	Fractional-order controller	Stability analysis

Advantages of using MPC are listed below.

- Using basic concepts of control in design
- Simple setting of the controller
- Ability to develop complex, non-minimum phase, and delayed systems
- Easy expansion capability for multiple-input and multiple-output systems
- To compensate for the naturally measurable disturbance effect of a controller It includes feedforward.
- Easy implementation of the control law
- Including control signal constraints, output, and state, in the design process (control optimal
- Very useful application for situations where the desired path is known in the future (robotics)

Disadvantages of using MPC are listed below.

- Control signal calculation is more complicated than classical controllers.
- Additional computational load for processes whose dynamics do not change.
- High calculation volume for bound controllers.
- Hardware cost to upgrade classic controllers to MPC and other advanced controllers.
- The need for a suitable model for the process.
- Impact of MPC benefits on the unavailability of the accurate model.
- The problem of proving stability and robustness in bound state and some non-linear systems.

MPC has been studied in several documented literature for the control of MRs [13], [32]. However, in most studies, the constraints are not considered. Also, the dynamic estimation is simple and cannot be used for real-world situations. Thus, the main contributions of the present paper are as follows.

- A new MPC strategy is introduced for MRs under both non-holonomic constraints and input restrictions.
- A T3-FLS based strategy is suggested for predictions and control for MRs with fully unknown dynamics.
- A chaotic-based path following is suggested, and it is shown that MRs well track a chaotic reference.
- Both experimental and simulation examinations are provided for evaluating the effectiveness of predictive strategy and FLS-based controller.

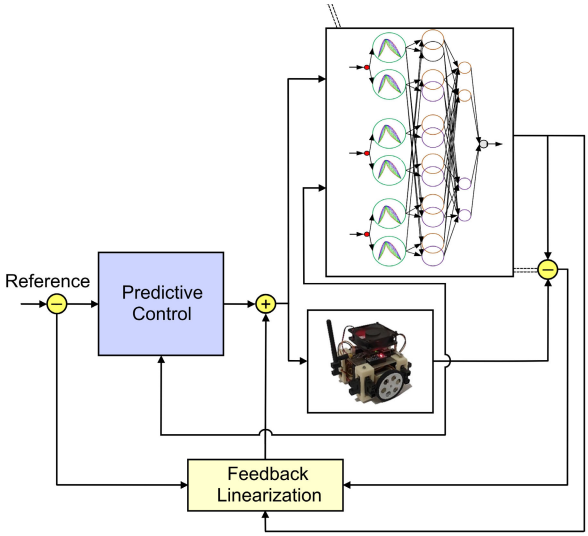

FIGURE 1. Control scheme.

The paper is organized as follows. A general view is given in Section II-A. The T3-FLS is described in Section II-B. The controller is designed and analyzed in Section II-C. The simulations and experimental studies are given in Section III. The main results are summarized in Section IV.

II. MATERIALS AND METHODS

A. GENERAL VIEW

The general equations of non-holonomic MRs are considered as [6], [9], and [33]:

$$\begin{aligned} \dot{z}_1 &= u_1 \\ \dot{z}_2 &= u_2 \\ \dot{z}_3 &= F(z) + z_2 u_1 + d \end{aligned} \tag{1}$$

where $z = [z_1, z_2, z_3]^T$, and $u_1, u_2 \in R$ represent control signals. $F(z)$ is a nonlinear function and $d \in R$ denotes the perturbation. $F(z) + d$ is approximated by the use of adaptive T3-FLS. So, the estimated system is written as:

$$\begin{aligned} \dot{z}_1 &= u_1 \\ \dot{z}_2 &= u_2 \\ \dot{z}_3 &= \text{T3-FLS}(z) + z_2 u_1 \end{aligned} \tag{2}$$

A general view of the schemed controller is given in Fig. 1.

B. TYPE-3 FLS

The dynamics are considered to be completely unknown, and as a result, the T3-FLS is utilized for online dynamic identification. T3-FLSs have been effectively employed in estimation and prediction applications. This paper introduces novel predictive controller using the T3-FLS model of MR. The T3-FLS is demonstrated in this section.

1) The inputs variables for T3-FLS are output and input of system in previous sample times. The general structure is given in Fig. 2.

2) Two membership functions are considered for input signals ($\tilde{\Omega}_i^j$, $i = 1, .., n$, $j = 1, 2$). The memberships are obtained as:

$$\bar{H}_{\tilde{\Omega}_{i\,|\bar{\alpha}_i}^j} = \begin{cases} 1 - \left(\dfrac{\left| x_i - C_{\tilde{\Omega}_i^j} \right|}{\underline{s}_{\tilde{\Omega}_i^j}} \right)^{\bar{\alpha}_i} & \text{if } C_{\tilde{\Omega}_i^j} - \underline{s}_{\tilde{\Omega}_i^j} < x_i \leq C_{\tilde{\Omega}_i^j} \\ 1 - \left(\dfrac{\left| x_i - C_{\tilde{\Omega}_i^j} \right|}{\bar{s}_{\tilde{\Omega}_i^j}} \right)^{\bar{\alpha}_i} & \text{if } C_{\tilde{\Omega}_i^j} < x_i \leq C_{\tilde{\Omega}_i^j} + \bar{s}_{\tilde{\Omega}_i^j} \\ 0 & \text{if } x_i > C_{\tilde{\Omega}_i^j} + \bar{s}_{\tilde{\Omega}_i^j} \text{ or } x_i \leq C_{\tilde{\Omega}_i^j} - \underline{s}_{\tilde{\Omega}_i^j} \end{cases} \tag{3}$$

$$\bar{H}_{\tilde{\Omega}_{i\,|\underline{\alpha}_i}^j} = \begin{cases} 1 - \left(\dfrac{\left| x_i - C_{\tilde{\Omega}_i^j} \right|}{\underline{s}_{\tilde{\Omega}_i^j}} \right)^{\underline{\alpha}_i} & \text{if } C_{\tilde{\Omega}_i^j} - \underline{s}_{\tilde{\Omega}_i^j} < x_i \leq C_{\tilde{\Omega}_i^j} \\ 1 - \left(\dfrac{\left| x_i - C_{\tilde{\Omega}_i^j} \right|}{\bar{s}_{\tilde{\Omega}_i^j}} \right)^{\underline{\alpha}_i} & \text{if } C_{\tilde{\Omega}_i^j} < x_i \leq C_{\tilde{\Omega}_i^j} + \bar{s}_{\tilde{\Omega}_i^j} \\ 0 & \text{if } x_i > C_{\tilde{\Omega}_i^j} + \bar{s}_{\tilde{\Omega}_i^j} \text{ or } x_i \leq C_{\tilde{\Omega}_i^j} - \underline{s}_{\tilde{\Omega}_i^j} \end{cases} \tag{4}$$

$$\underline{H}_{\tilde{\Omega}_{i\,|\bar{\alpha}_i}^j} = \begin{cases} 1 - \left(\dfrac{\left| x_i - C_{\tilde{\Omega}_i^j} \right|}{\underline{s}_{\tilde{\Omega}_i^j}} \right)^{\frac{1}{\bar{\alpha}_i}} & \text{if } C_{\tilde{\Omega}_i^j} - \underline{s}_{\tilde{\Omega}_i^j} < x_i \leq C_{\tilde{\Omega}_i^j} \\ 1 - \left(\dfrac{\left| x_i - C_{\tilde{\Omega}_i^j} \right|}{\bar{s}_{\tilde{\Omega}_i^j}} \right)^{\frac{1}{\bar{\alpha}_i}} & \text{if } C_{\tilde{\Omega}_i^j} < x_i \leq C_{\tilde{\Omega}_i^j} + \bar{s}_{\tilde{\Omega}_i^j} \\ 0 & \text{if } x_i > C_{\tilde{\Omega}_i^j} + \bar{s}_{\tilde{\Omega}_i^j} \text{ or } x_i \leq C_{\tilde{\Omega}_i^j} - \underline{s}_{\tilde{\Omega}_i^j} \end{cases} \tag{5}$$

$$\underline{H}_{\tilde{\Omega}_{i\,|\underline{\alpha}_i}^j} = \begin{cases} 1 - \left(\dfrac{\left| x_i - C_{\tilde{\Omega}_i^j} \right|}{\underline{s}_{\tilde{\Omega}_i^j}} \right)^{\frac{1}{\underline{\alpha}_i}} & \text{if } C_{\tilde{\Omega}_i^j} - \underline{s}_{\tilde{\Omega}_i^j} < x_i \leq C_{\tilde{\Omega}_i^j} \\ 1 - \left(\dfrac{\left| x_i - C_{\tilde{\Omega}_i^j} \right|}{\bar{s}_{\tilde{\Omega}_i^j}} \right)^{\frac{1}{\underline{\alpha}_i}} & \text{if } C_{\tilde{\Omega}_i^j} < x_i \leq C_{\tilde{\Omega}_i^j} + \bar{s}_{\tilde{\Omega}_i^j} \\ 0 & \text{if } x_i > C_{\tilde{\Omega}_i^j} + \bar{s}_{\tilde{\Omega}_i^j} \text{ or } x_i \leq C_{\tilde{\Omega}_i^j} - \underline{s}_{\tilde{\Omega}_i^j} \end{cases} \tag{6}$$

where, $\bar{H}_{\tilde{\Omega}_{i\,|\bar{\alpha}_i}^j}/\bar{H}_{\tilde{\Omega}_{i\,|\underline{\alpha}_i}^j}$ and $\underline{H}_{\tilde{\Omega}_{i\,|\bar{\alpha}_i}^j}/\underline{H}_{\tilde{\Omega}_{i\,|\underline{\alpha}_i}^j}$ are the upper/lower memberships for $\tilde{\Omega}_i^j$ at $\underline{\alpha}_i$ and $\bar{\alpha}_i$. $C_{\tilde{\Omega}_i^j}$, are the center of $C_{\tilde{\Omega}_i^j}$, and $\underline{s}_{\tilde{\Omega}_i^j}$ and $\bar{s}_{\tilde{\Omega}_i^j}$ are constants (see Fig. 3).

3) The upper rule firings $\bar{\mu}_{\bar{\alpha}_i}^l$, $\bar{\mu}_{\underline{\alpha}_i}^l$, and lower firings $\underline{\mu}_{\bar{\alpha}_i}^l$ and $\underline{\mu}_{\underline{\alpha}_i}^l$ are written as:

$$\bar{\mu}_{\bar{\alpha}_i}^l = \bar{H}_{\tilde{\Omega}_{1\,|\bar{\alpha}_i}^{p_1}} \cdot \bar{H}_{\tilde{\Omega}_{1\,|\bar{\alpha}_i}^{p_2}} \cdots \bar{H}_{\tilde{\Omega}_{1\,|\bar{\alpha}_i}^{p_n}} \tag{7}$$

$$\bar{\mu}_{\underline{\alpha}_i}^l = \bar{H}_{\tilde{\Omega}_{1\,|\underline{\alpha}_i}^{p_1}} \cdot \bar{H}_{\tilde{\Omega}_{1\,|\underline{\alpha}_i}^{p_2}} \cdots \bar{H}_{\tilde{\Omega}_{1\,|\underline{\alpha}_i}^{p_n}} \tag{8}$$

$$\underline{\mu}_{\bar{\alpha}_i}^l = \underline{H}_{\tilde{\Omega}_{1\,|\bar{\alpha}_i}^{p_1}} \cdot \underline{H}_{\tilde{\Omega}_{1\,|\bar{\alpha}_i}^{p_2}} \cdots \underline{H}_{\tilde{\Omega}_{1\,|\bar{\alpha}_i}^{p_n}} \tag{9}$$

$$\underline{\mu}_{\underline{\alpha}_i}^l = \underline{H}_{\tilde{\Omega}_{1\,|\underline{\alpha}_i}^{p_1}} \cdot \underline{H}_{\tilde{\Omega}_{1\,|\underline{\alpha}_i}^{p_2}} \cdots \underline{H}_{\tilde{\Omega}_{1\,|\underline{\alpha}_i}^{p_n}} \tag{10}$$

The output fuzzy system f is written as [31]:

$$f = \frac{\sum_{i=1}^{n_\alpha} \left(\underline{\alpha}_i \underline{\ell}_i + \bar{\alpha}_i \bar{\ell}_i \right)}{\sum_{i=1}^{n_\alpha} \left(\underline{\alpha}_i + \bar{\alpha}_i \right)} \tag{11}$$

where,

$$\bar{\ell}_i = \frac{\sum_{l=1}^{n_r} \left(\bar{\mu}_{\bar{\alpha}_i}^l \bar{\vartheta}_{l,\bar{\alpha}_i} + \underline{\mu}_{\bar{\alpha}_i}^l \underline{\vartheta}_{l,\bar{\alpha}_i} \right)}{\sum_{l=1}^{n_r} \left(\bar{\mu}_{\bar{\alpha}_i}^l + \underline{\mu}_{\bar{\alpha}_i}^l \right)} \tag{12}$$

$$\underline{\ell}_i = \frac{\sum_{l=1}^{n_r} \left(\bar{\mu}_{\underline{\alpha}_i}^l \bar{\vartheta}_{l,\underline{\alpha}_i} + \underline{\mu}_{\underline{\alpha}_i}^l \underline{\vartheta}_{l,\underline{\alpha}_i} \right)}{\sum_{l=1}^{n_r} \left(\bar{\mu}_{\underline{\alpha}_i}^l + \underline{\mu}_{\underline{\alpha}_i}^l \right)} \tag{13}$$

The output of fuzzy system f is rewritten as:

$$f(X, \vartheta) = \vartheta^T \beta \tag{14}$$

where,

$$\begin{aligned} \beta^T = \Big[& \underline{\beta}_{1,\underline{\alpha}_i}, \ldots, \underline{\beta}_{n_r,\underline{\alpha}_i}, \\ & \underline{\beta}_{1,\bar{\alpha}_i}, \ldots, \underline{\beta}_{n_r,\bar{\alpha}_i}, \\ & \bar{\beta}_{1,\underline{\alpha}_i}, \ldots, \bar{\beta}_{n_r,\underline{\alpha}_i}, \\ & \bar{\beta}_{1,\bar{\alpha}_i}, \ldots, \bar{\beta}_{n_r,\bar{\alpha}_i} \Big] \end{aligned} \tag{15}$$

$$\begin{aligned} \vartheta^T = \Big[& \underline{\vartheta}_{1,\underline{\alpha}_i}, \ldots, \underline{\vartheta}_{n_r,\underline{\alpha}_i}, \\ & \underline{\vartheta}_{1,\bar{\alpha}_i}, \ldots, \underline{\vartheta}_{n_r,\bar{\alpha}_i}, \\ & \bar{\vartheta}_{1,\underline{\alpha}_i}, \ldots, \bar{\vartheta}_{n_r,\underline{\alpha}_i}, \\ & \bar{\vartheta}_{1,\bar{\alpha}_i}, \ldots, \bar{\vartheta}_{n_r,\bar{\alpha}_i} \Big] \end{aligned} \tag{16}$$

$$\underline{\beta}_{l,\underline{\alpha}_i} = \frac{\sum_{i=1}^{n_\alpha} \underline{\alpha}_i \underline{\mu}_{\underline{\alpha}_i}^l}{\sum_{i=1}^{n_\alpha} \left(\underline{\alpha}_i + \bar{\alpha}_i \right) \sum_{l=1}^{n_r} \left(\bar{\mu}_{\underline{\alpha}_i}^l + \underline{\mu}_{\underline{\alpha}_i}^l \right)} \tag{17}$$

$$\bar{\beta}_{l,\underline{\alpha}_i} = \frac{\sum_{i=1}^{n_\alpha} \underline{\alpha}_i \bar{\mu}_{\underline{\alpha}_i}^l}{\sum_{i=1}^{n_\alpha} \left(\underline{\alpha}_i + \bar{\alpha}_i \right) \sum_{l=1}^{n_r} \left(\bar{\mu}_{\underline{\alpha}_i}^l + \underline{\mu}_{\underline{\alpha}_i}^l \right)} \tag{18}$$

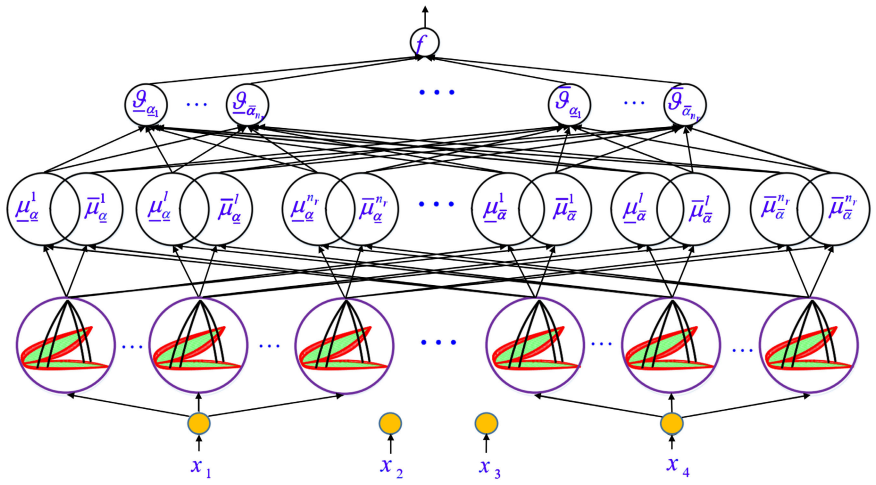

FIGURE 2. The T3-FLS structure.

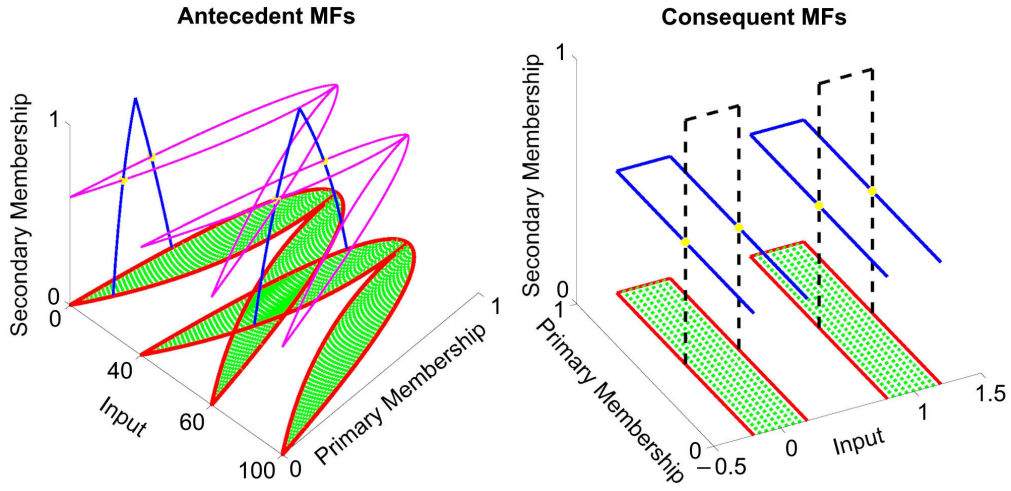

FIGURE 3. Type-3 MF.

$$\underline{\beta}_{l,\bar{\alpha}} = \frac{\sum_{i=1}^{n_\alpha} \bar{\alpha}_i \underline{\mu}_{\bar{\alpha}}^{l}}{\sum_{i=1}^{n_\alpha} \left(\underline{\alpha}_i + \bar{\alpha}_i\right) \sum_{l=1}^{n_r} \left(\bar{\mu}_{\bar{\alpha}}^{l} + \underline{\mu}_{\bar{\alpha}}^{l}\right)} \tag{19}$$

$$\bar{\beta}_{l,\bar{\alpha}} = \frac{\sum_{i=1}^{n_\alpha} \bar{\alpha}_i \bar{\mu}_{\bar{\alpha}}^{l}}{\sum_{i=1}^{n_\alpha} \left(\underline{\alpha}_i + \bar{\alpha}_i\right) \sum_{l=1}^{n_r} \left(\bar{\mu}_{\bar{\alpha}}^{l} + \underline{\mu}_{\bar{\alpha}}^{l}\right)} \tag{20}$$

C. CONTROL METHOD

In general, this algorithm, which belongs to controllers based on the model, is a generalization of the methods of pole placement and LQ optimal control; Besides eliminating their weak points as much as possible and due to being resistant, its greater ability is confirmed. In addition, in multivariable processes where decoupling conditions are established, by applying the predictive controller, different basic paths can be optimally followed for each of the outputs and unwanted disturbances in the output can be removed. Predictive controllers are implemented in the time domain and are effective for controlling many types of systems, from simple dynamic systems to the most complex ones. In general, a predictive controller is a controller that operates based on the following principles:

- Using a model to predict the future outputs of the system in a limited period of time (prediction horizon).
- Definition of an objective function, which is usually a linear combination of the error and control signal changes.
- Optimizing the objective function in order to find the desired control signals.
- Apply the control signal obtained for the current moment to the system and repeat the calculations for the next moments.

The impulse response model, step response, transformation function, and state space are common models for predicting system output. The objective function is chosen on the basis that the future output of the system follows a desired reference signal in the prediction horizon and at the same time the control signal changes are minimal. Usually, a first-order filter is used to smooth the reference signal and determine the desired output. In some methods, the changes of the control signal are not taken into account, so some other values of the control signal itself are considered instead of its changes. Generally, there are restrictions on control signals and system outputs that must be considered in the optimization of the criterion function. In the forecasting horizon, p future steps are examined and in each calculation, the output of the system is calculated up to the first step p. Control strategy in the MPC controllers has the following steps.

1) First step:
   - Determine the prediction horizon N
   - Calculation of forecast outputs $y(t+k|t)$ for $k = 1, \ldots, N$ depends on two parts:
     - The part dependent on the known values of the past time of input and output
     - The part dependent on the control signal in the future time $u(t+k|t)$ for $k = 0, \ldots, N-1$.
2) Second step:
   - Calculation of the control signal based on the optimization of an objective function (reducing the reference trajectory tracking error $w(t+k)$)
   - Choosing a square form for optimization criteria (including tracking error, control signal size)
   - Closed form for u: in linear system conditions, without constraints and quadratic optimization criteria.
3) Third step:
   - Only $u(t|t)$ is applied to the system.
   - At the moment $t+1$, with the new information $y(t+1)$, the control signal is recalculated (restarting from the first step)

A third-order non-holonomic system is considered as:

$$\begin{aligned} \dot{x}_1 &= u_1 \\ \dot{x}_2 &= u_2 \\ \dot{x}_3 &= f(x) + x_2 u_1 + d \end{aligned} \tag{21}$$

The controller is designed for (21) such that the stability is ensured. The control law is obtained in such a way that if the initial conditions of the system are acceptable anywhere in the space (Ω). Then this control law will bring the system to the equilibrium point. First, the feedback linearization is applied as:

$$u_1 = \frac{-\hat{f}(x) + V + \alpha x_1}{x_2} \tag{22}$$

where $\hat{f}(x)$ represents T3-FLS. Then we have:

$$\begin{aligned} \dot{x}_1 &= u_1 \\ \dot{x}_2 &= u_2 \\ \dot{x}_3 &= V + \alpha x_1 \end{aligned} \tag{23}$$

where

$$\dot{Z} = \begin{bmatrix} 0 & 0 & 0 \\ 0 & 0 & 0 \\ \alpha & 0 & 0 \end{bmatrix} Z + \begin{bmatrix} 1 & 0 & 0 \\ 0 & 1 & 0 \\ 0 & 0 & 1 \end{bmatrix} \begin{bmatrix} u_1 \\ u_2 \\ V \end{bmatrix} \tag{24}$$

The dynamics are written as:

$$\begin{bmatrix} \dot{Z}_1 \\ \dot{Z}_2 \\ \dot{Z}_3 \end{bmatrix} = \begin{bmatrix} 0 & 0 & 0 \\ 0 & 0 & 0 \\ \alpha & 0 & 0 \end{bmatrix} \begin{bmatrix} Z_1 \\ Z_2 \\ Z_3 \end{bmatrix} + \begin{bmatrix} 1 & 0 & 0 \\ 0 & 1 & 0 \\ 0 & 0 & 1 \end{bmatrix} \begin{bmatrix} u_1 \\ u_2 \\ V \end{bmatrix} \tag{25}$$

By applying the controller, we can write:

$$\begin{aligned} \dot{x}_1 &= u_1 \\ \dot{x}_2 &= u_2 \\ \dot{x}_3 &= \alpha Z_1 + V \end{aligned} \tag{26}$$

where

$$A = \begin{bmatrix} 0 & 0 & 0 \\ 0 & 0 & 0 \\ \alpha & 0 & 0 \end{bmatrix}, \; B = \begin{bmatrix} 1 & 0 & 0 \\ 0 & 1 & 0 \\ 0 & 0 & 1 \end{bmatrix}, \; C = \begin{bmatrix} 1 & 0 & 0 \\ 0 & 1 & 0 \\ 0 & 0 & 1 \end{bmatrix} \tag{27}$$

In discrete form, (27) is written as:

$$\begin{aligned} x_{t+1} &= A_d(x) x_t + B_d u_t + D \\ y_{t+1} &= C_d x_{t+1} \end{aligned} \tag{28}$$

The matrices A_d, B_d, C_d are considered as:

$$\begin{aligned} A_d &= e^{AT} \approx I + AT \\ B_d &= \int_0^{\tau} e^{AT} B d\tau \approx BT \\ C_d &= C \end{aligned} \tag{29}$$

where T denotes the sampling period. Considering T, we can write:

$$\begin{aligned} A_d &= \begin{bmatrix} 1 & 0 & 0 \\ 0 & 1 & 0 \\ 0 & 0 & 1 \end{bmatrix} + \begin{bmatrix} 0 & 0 & 0 \\ 0 & 0 & 0 \\ \alpha & 0 & 0 \end{bmatrix} * T, \quad D_d = \begin{bmatrix} 0 \\ 0 \\ d \end{bmatrix} * T \\ B_d &= \begin{bmatrix} 1 & 0 & 0 \\ 0 & 1 & 0 \\ 0 & 0 & 1 \end{bmatrix} * T, \quad C_d = \begin{bmatrix} 1 & 0 & 0 \\ 0 & 1 & 0 \\ 0 & 0 & 1 \end{bmatrix}. \end{aligned} \tag{30}$$

The following equations are used for prediction:

$$\begin{aligned} x_{k+1} &= \tilde{A} x_k + \tilde{B} \Delta u_k + \tilde{D} \\ y_{k+1} &= \tilde{C} x_{k+1} \end{aligned} \tag{31}$$

where

$$\tilde{A} = \begin{bmatrix} A_d & B_d \\ 0_{p \times n} & I_{p \times p} \end{bmatrix} \qquad \tilde{B} = \begin{bmatrix} B_d \\ I_{p \times p} \end{bmatrix}$$

$$\tilde{C} = \begin{bmatrix} C_d & 0_{q\times p} \end{bmatrix} \qquad \tilde{D} = \begin{bmatrix} D \\ 0_{p\times 1} \end{bmatrix}$$
$$x_k^T = \begin{bmatrix} x_k^T & u_{k-1}^T \end{bmatrix} \tag{32}$$

where p denotes the number of inputs, q and n denote output and states numbers, and for other matrices we have:

$$\begin{aligned} \tilde{D} &\in R^{[(n+p)\times 1]} \\ \tilde{A} &\in R^{[(n+p)\times(n+p)]} \\ \tilde{C} &\in R^{[q\times(n+p)]} \\ \tilde{B} &\in R^{[(n+p)\times p]} \end{aligned} \tag{33}$$

The prediction horizon of output/control are shown by n_y/n_u. By the use of (31) the n-step ahead is predicted as follows:

$$\begin{aligned} &x_{k+n} \\ &= \tilde{A}^n x_k + \tilde{A}^{n-1}\tilde{B}\,\Delta u_k + \ldots + \tilde{B}u_{k+n-1} + \tilde{A}^{n-1}\tilde{D} + \tilde{D} \\ y_{k+n} &= \tilde{C}\,x_{k+n} \end{aligned} \tag{34}$$

The predicted output is written as:

$$\hat{y} = \xi'\,\hat{x} + \xi''\,\Delta u + \xi'''\,d \tag{35}$$

where

$$\Delta u^T = \begin{bmatrix} u_k & u_{k+1} & \cdots & u_{k+n-1} \end{bmatrix} \tag{36}$$
$$\hat{y} = \begin{bmatrix} y_{k+1} & y_{k+2} & \cdots & y_{k+n_y} \end{bmatrix} \tag{37}$$
$$\xi' \in R^{(n_y q)\times n},\ \xi'' \in R^{(n_y q)\times(n_u p)},\ \xi''' \in R^{(n_y q)\times(n_y n)} \tag{38}$$

where $\hat{y} \in R^{(n_y q)\times 1}$ is the vector of predicted output, $\hat{x} \in R^{n_y n+p}$ is the estimated states using Kalman filter, $\Delta u \in R^{n_u p\times 1}$ represents the changes of control input, and d is the disturbance. ξ', ξ'' and ξ''' are written as:

$$\xi' = \begin{bmatrix} \tilde{C}\tilde{A} & \tilde{C}\tilde{A}^2 & \cdots & \tilde{C}\tilde{A}^{n_y} \end{bmatrix}^T \tag{39}$$

$$\xi'' = \begin{bmatrix} \tilde{C}\tilde{B} & 0 & 0 & \cdots & 0 \\ \tilde{C}\tilde{A}\tilde{B} & \tilde{C}\tilde{B} & 0 & \cdots & 0 \\ \tilde{C}\tilde{A}^2\tilde{B} & \tilde{C}\tilde{A}\tilde{B} & \tilde{C}\tilde{B} & \cdots & 0 \\ \tilde{C}\tilde{A}^{n_y-1}\tilde{B} & \tilde{C}\tilde{A}^{n_y-2}\tilde{B} & \cdots & \cdots & \tilde{C}\tilde{B} \end{bmatrix} \tag{40}$$

$$\xi''' = \begin{bmatrix} \tilde{C} & 0 & 0 & \cdots & 0 \\ \tilde{C}\tilde{A} & \tilde{C} & 0 & \cdots & 0 \\ \tilde{C}\tilde{A}^2 & \tilde{C}\tilde{A} & \tilde{C} & \cdots & 0 \\ \tilde{C}\tilde{A}^{n_y-1} & \tilde{C}\tilde{A}^{n_y-2} & \cdots & \cdots & \tilde{C} \end{bmatrix} \tag{41}$$

To derive the control signal, the cost function (42) is minimized:

$$\begin{aligned} J = {} & \Delta u^T W_u \Delta u \\ & + (w-\hat{y})^T W_y (w-\hat{y}) \end{aligned} \tag{42}$$

where $w \in R^{(n_y q)\times 1}$ is the vector of reference in future times, $W_y \in R^{(n_y q)\times(n_y q)}$ is positive definite matrix that represents the importance of tracking error, and $W_u \in R^{n_u\times n_u}$ is positive definite matrix that shows the importance of control effort. The matrices ξ', ξ'', and ξ''' are updated in each sample. By replacing $\hat{y}$ form (35) into (42), Δu is obtained as:

$$\Delta u = \left(\xi''^T W_y \xi'' + W_u\right)^{-1} \xi''^T W_y \left(w - \xi' x - \xi''' d\right) \tag{43}$$

To consider the constraints on inputs and outputs, the cost function is written as:

$$\begin{aligned} J = {} & (y_{t+1\backslash t} - r_{t+1\backslash t})^T Q\,(y_{t+1\backslash t} - r_{t+1\backslash t}) \\ & + \Delta u_{t\backslash t}{}^T R\,\Delta u_{t\backslash t} + u_{t\backslash t}{}^T R_2\,u_{t\backslash t} \end{aligned} \tag{44}$$

where

$$\min_{\Delta u_{t\backslash t}} \ J \tag{45}$$

$$\begin{aligned} & u_{t|t}^{\min} \le u_{t|t} \le u_{t|t}^{\max} \\ & \Delta u_{t|t}^{\min} \le \Delta u_{t|t} \le \Delta u_{t|t}^{\max} \\ & y_{t+1|t}^{\min} \le y_{t+1|t} \le y_{t+1|t}^{\max} \end{aligned} \tag{46}$$

The constraints on magnitude of input control are written as:

$$\begin{bmatrix} I \\ -I \end{bmatrix} u_{t\backslash t} \le \begin{bmatrix} u_{\max} \\ -u_{\min} \end{bmatrix} \tag{47}$$

To formulate the constraint $\Delta u_{\min} \le \Delta u_{t\backslash t} \le \Delta u_{\max}$, we can write:

$$u_{t\backslash t} = s\,\Delta u_{t\backslash t} + c\,u_{t-1} \tag{48}$$

where

$$\Delta u_{t\backslash t} = s^{-1}\,u_{t\backslash t} + s^{-1} c\,u_{t-1} \tag{49}$$

The constraint $y_{\min} \le y_{t+1\backslash t} \le y_{\max}$ is written as:

$$y_{t+1\backslash t} = p_t + F_t\,\Delta u_{t\backslash t} \tag{50}$$

It can be also simplified as

$$y_{t+1\backslash t} = p_t + F_t\,u_{t\backslash t} \tag{51}$$

Then we can write:

$$\begin{bmatrix} F_t \\ -F_t \end{bmatrix} u_{t\backslash t} \le \begin{bmatrix} y_{\max} - p_t \\ -y_{\min} + p_t \end{bmatrix} \tag{52}$$

The constraints above are written as:

$$A\,u_{t\backslash t} \le b \tag{53}$$

TABLE 2. Simulation conditions.

Parameter	Value
p	3
n	3
q	3
T	0.02
α	2
$C_{\tilde{\Omega}_i^1}$	-1
$C_{\tilde{\Omega}_i^2}$	1
$\bar{s}_{\tilde{\Omega}_i^j}$	2
$\underline{s}_{\tilde{\Omega}_i^j}$	2
$\bar{\alpha}_i$	2
$\underline{\alpha}_i$	0.5

The matrices A and b are obtained as:

$$A = \begin{bmatrix} s \\ -s \\ I \\ -I \\ F_t \\ -F_t \end{bmatrix}, \quad b = \begin{bmatrix} u_{t\backslash t}^{\max} - c\,u_{t-1} \\ u_{t\backslash t}^{\min} + c\,u_{t-1} \\ \Delta u_{t\backslash t}^{\max} \\ \Delta u_{t\backslash t}^{\min} \\ y_{t+1\backslash t}^{\max} - p_t \\ y_{t+1\backslash t}^{\min} + p_t \end{bmatrix} \tag{54}$$

The relation between $\Delta u_{t\backslash t}$ and $u_{t\backslash t}$ is written as:

$$u_{t\backslash t} = s\,\Delta u_{t\backslash t} + c\,u_{t-1} \tag{55}$$

where

$$s = \begin{bmatrix} I & 0 & 0 & \cdots & 0 \\ I & I & 0 & \cdots & 0 \\ \vdots & \vdots & \vdots & \vdots & \vdots \\ I & I & I & \cdots & I \end{bmatrix}, \quad c = \begin{bmatrix} I \\ I \\ \vdots \\ I \end{bmatrix} \tag{56}$$

Equation (55) is written as:

$$\Delta u_{t\backslash t} = s_2\,\Delta u_{t\backslash t} + c_2\,u_{t-1} \tag{57}$$

where

$$s = \begin{bmatrix} I & 0 & 0 & \cdots & 0 \\ -I & I & 0 & \cdots & 0 \\ 0 & -I & I & \vdots & 0 \\ \vdots & \vdots & \vdots & \cdots & \vdots \\ 0 & 0 & 0 & \cdots & -I \end{bmatrix}, \quad c = \begin{bmatrix} I \\ 0 \\ \vdots \\ 0 \end{bmatrix} \tag{58}$$

Considering $s_2 = s^{-1}$ and $c_2 = s^{-1}c$, we can write:

$$u_{t-1|t} = (I - s_2)\,u_{t|t} + c_2\,u_{t-1} \tag{59}$$

The prediction model is considered as:

$$u_{t+1|t} = p_t + F_t \Delta u_{t|t} \tag{60}$$

where p_t is a part of past outputs and inputs, and F_t is constant matrix.

III. RESULTS AND DISCUSSION

In this section, the designed predictive controller is evaluated. The effect of uncertainties and constraints is investigated. An augmented model based on (31) and (32) is constructed for the plant, and the by prediction of output signals the control input is obtained. The system parameters are considered as given in Table 2.

A. NON-CONSTRAINED CONDITION

For the first scenario, it is assumed that there are no constraints on outputs and input signals. This means that the system is free to move and respond to any changes in the environment without any limitations. The trajectories of x_1, x_2 and x_3 are depicted in Fig. 4.

As can be seen, all the states with different initialization, in a limited time and with a high convergence speed, track the desired path and converge without any overshoot. The control signals are shown in Fig. 5. It can be seen that all input signals are smooth and implementable, with no fluctuations. This indicates that the system is stable and robust, and can respond to any changes in the environment without any issues.

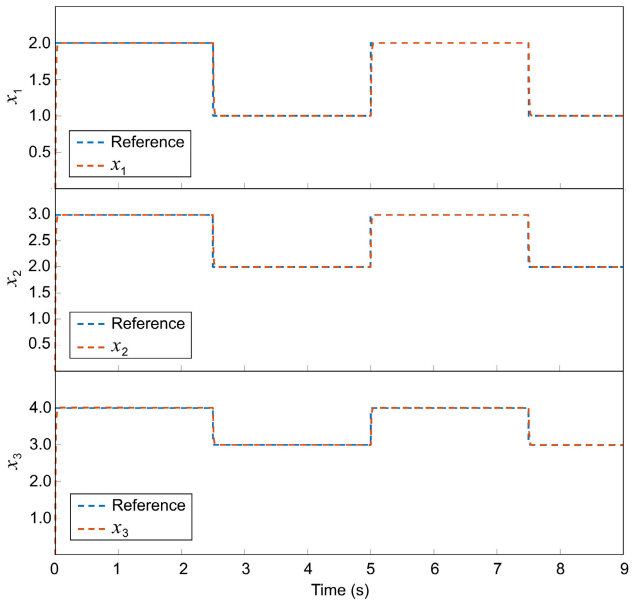

FIGURE 4. Trajectories of x_1, x_2, and x_3 for the non-constrained case.

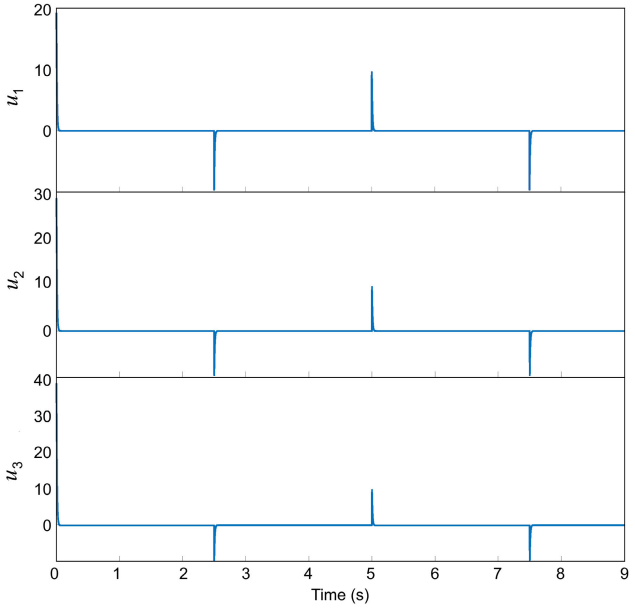

FIGURE 5. Trajectories of u_1, u_2, and u_3 for the non-constrained case.

B. CONSTRAINED CONDITION

For the second scenario, we consider the following constraints:

$$-2 \leq u \leq 2 \tag{61}$$

The trajectories of x_1, x_2 and x_3 are depicted in Fig. 6. As can be seen, all the states with different initialization, in a short time are converged to the desired path there is no overshoot

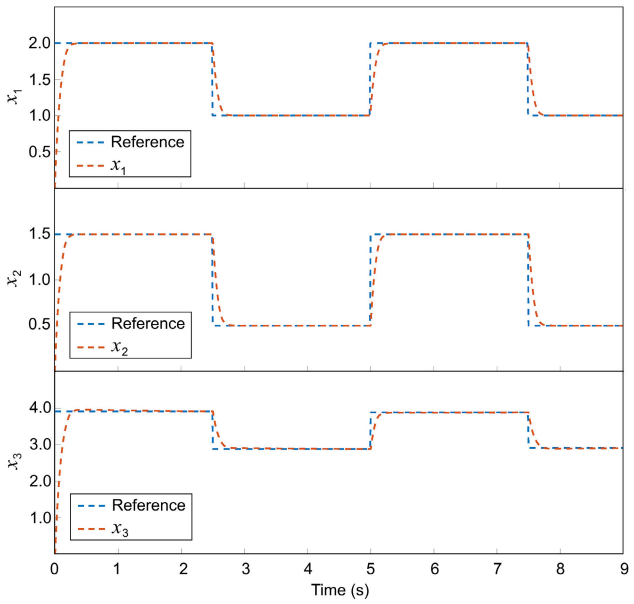

FIGURE 6. Constrained case: Trajectories of x_1, x_2, & x_3.

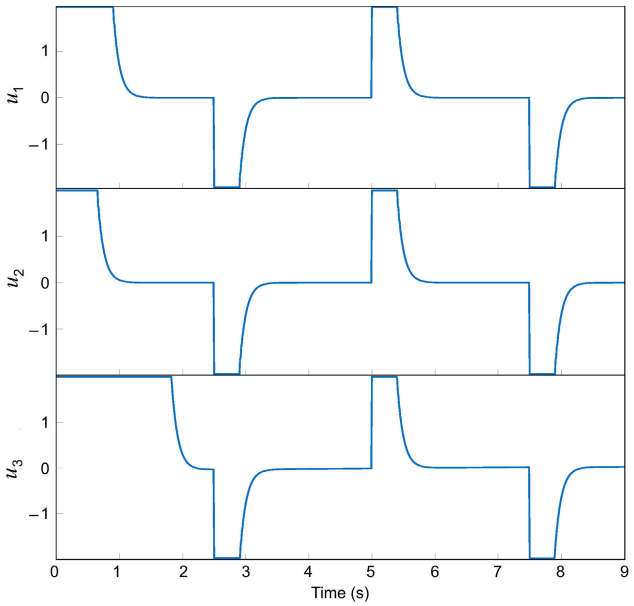

FIGURE 7. Constrained case: Trajectories of u_1, u_2, & u_3.

in signals. The control signals are shown in Fig. 7. It can be seen that all input signals are between the constraints, and the signals are smooth and implementable, with no fluctuations. This indicates that the system is stable and robust, and can respond to any changes in the environment without any issues.

To better see the superiorly of type-3 FLS-based controller a comparison is carried out with some other types of fuzzy controllers such as type-1 fuzzy-based SMC [17] and type-2 fuzzy-based SMC [16]. In these methods, the stability is analyzed using the SMC theorem and they are applied to the MR systems. The comparisons in Table 3 show that the suggested scheme along with the theory of powerful T3-FLS

TABLE 3. Comparison of RMSE.

	Output		
	x_1	x_2	x_3
Type-1 fuzzy based SMC [17]	1.3157	1.0981	1.5175
Type-2 fuzzy based SMC [16]	1.2871	0.2107	0.1289
Proposed Method	0.0124	0.0257	0.0791

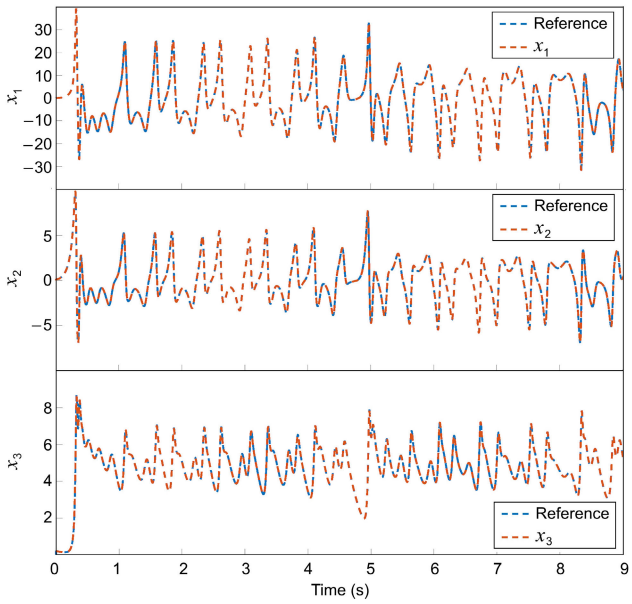

FIGURE 8. Chaotic reference: Trajectories of x_1, x_2, & x_3.

results in a more accurate response. The outputs well follow the reference signals.

C. CHAOTIC REFERENCE

For the third scenario, the reference is assumed to be a chaotic signal. For outputs x_1, x_2 and x_3 the references are considered to be x_{11}, x_{12} and x_{13} that are generated by the following equations.

$$\begin{cases} \dot{x}_{11} = 35x_{12}x_{13} + 35\,(x_{12} - x_{11}) \\ \dot{x}_{12} = -5x_{11}x_{13}25x_{11} + x_{12} + x_{14} \\ \dot{x}_{13} = x_{11}x_{12} - 4x_{13} \\ \dot{x}_{14} = -100x_{12} \end{cases} \tag{62}$$

The trajectories of x_1, x_2 and x_3 are depicted in Fig. 8. The phase portraits are depicted in Fig. 9. The outputs track the chaotic references very well. The plots in Fig. 9 show that the outputs closely follow the chaotic references, indicating that the proposed control scheme is effective in tracking unpredictable paths. The stochastic nature of the reference path makes it difficult to predict, which is

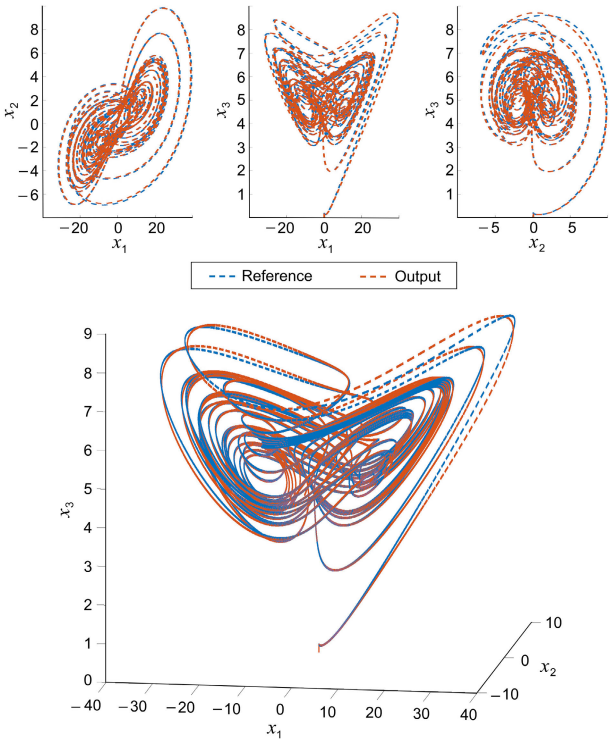

FIGURE 9. Chaotic reference: Phase portrait in 2D (top panels) and 3D (the bottom panel) dimensions.

a desirable feature for secure patrol robotic applications. The control signals are shown in Fig. 10. Similar to the previous examinations, the controller inputs are smooth and implementable. These findings suggest that the introduced scheme can be employed to a wide range of plants with unpredictable dynamics, making it a promising approach for various real-world applications.

D. EXPERIMENT

The suggested controller is applied on a practical robot (see Fig. 11). The robot communicates with the laptop is a radio module called NRF24L01. This module uses GFSK modulation and has a frequency of 2.4 GHz, making it easier to transmit signals through walls and other objects. It can transmit heavy data such as audio or video at a maximum rate of 2 MB per second. The laptop receiver is connected to a microcontroller using the SPI protocol, which is then connected to the laptop through a USB to serial converter. MATLAB software communicates with the microcontroller through a virtual serial port with a baud rate of 9600. The robot's microcontroller is also connected to the NRF24L01 module using the SPI protocol, as well as Sharp sensors. The same microcontroller is connected to the motor controller using UART serial communication. An angular acceleration sensor is also connected to the motor controller using the I2C protocol. The motor drivers have three control pins: EN, direction, and pulse/step, which rotate the motor one step for

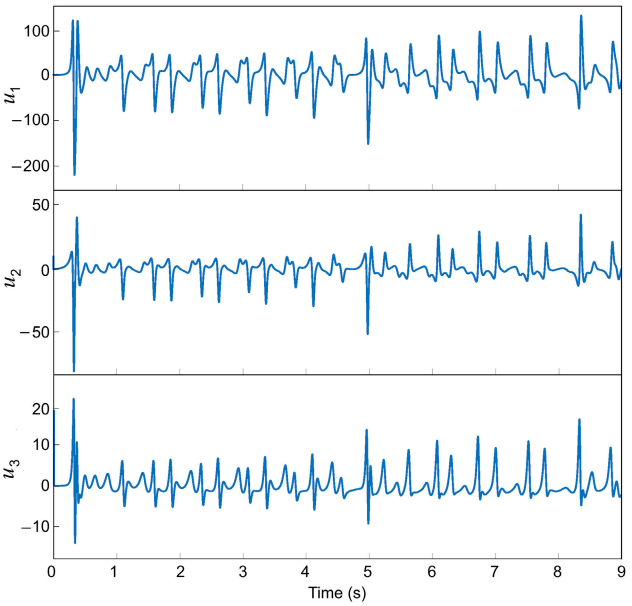

FIGURE 10. Chaotic reference: Trajectories of u_1, u_2, & u_3.

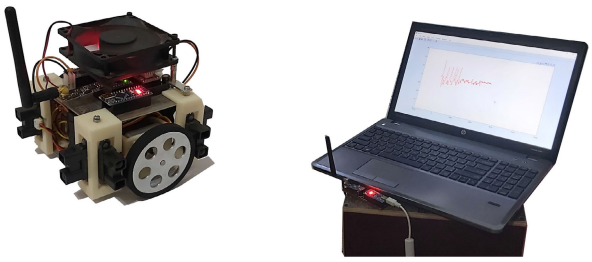

FIGURE 11. Experiment: Implementation setup.

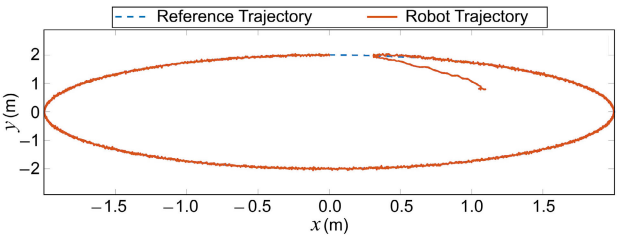

FIGURE 12. Experiment: Path tracking performance.

each pulse received. The performance of path following is given in Fig. 12. It is seen that the suggested controller has a good efficiency in real-world situations.

The estimation part of this paper can be developed using other intelligent systems, and other modeling approaches like, hybrid modeling approach [11], non-singular control systems [16], and new decision-making based modeling systems [10].

IV. CONCLUSION

In this paper, a new control scheme is applied for MRs. Besides the non-holonomic constraints, some other

restrictions are also considered in input control. Also, the dynamics are supposed to be entirely unknown. A T3-FLS is developed for the estimation of unknown dynamics. Three simulation examples and one practical experiment are provided to show the designed controller's effectiveness. In the first example, the controller is applied to a plant with non-holonomic constraints with unknown dynamics. It is shown that the suggested controller results in an accurate response without overshoot, and with smooth control signals. In the second example, the controller is applied to a plant with non-holonomic constraints with unknown dynamics and input constraints. Similarly, the results show that even in spite of complex constraints and perturbations the suggested controller well tracks a pulse reference. In the third simulation example, the reference signal is considered to be a chaotic reference. All reference signals of the outputs are generated by a chaotic system. The results show that the system well tracks the chaotic path and demonstrates that the designed controller can be applied for secure robotic parol applications. Finally, in the experimental examination, the suggested controller is applied to a real MR, and it is shown that MR follows a designed path with acceptable accuracy.

REFERENCES

[1] A. A. AbuBaker and Y. Y. Ghadi, "Optimization of fuzzy rules using neural network to control mobile robot in non-structured environment," *Bull. Electr. Eng. Informat.*, vol. 12, no. 5, pp. 2777–2783, Oct. 2023.

[2] S.-D. Achirei, R. Mocanu, A.-T. Popovici, and C.-C. Dosoftei, "Model-predictive control for omnidirectional mobile robots in logistic environments based on object detection using CNNs," *Sensors*, vol. 23, no. 11, p. 4992, May 2023.

[3] A. S. Alkabaa, O. Taylan, M. Balubaid, C. Zhang, and A. Mohammadzadeh, "A practical type-3 fuzzy control for mobile robots: Predictive and Boltzmann-based learning," *Complex Intell. Syst.*, vol. 9, no. 6, pp. 6509–6522, Dec. 2023.

[4] L. Amador-Angulo, O. Castillo, P. Melin, and J. R. Castro, "Interval type-3 fuzzy adaptation of the bee colony optimization algorithm for optimal fuzzy control of an autonomous mobile robot," *Micromachines*, vol. 13, no. 9, p. 1490, Sep. 2022.

[5] A. Azzabi and K. Nouri, "Design of a robust tracking controller for a nonholonomic mobile robot based on sliding mode with adaptive gain," *Int. J. Adv. Robotic Syst.*, vol. 18, no. 1, pp. 1–18, Jan. 2021.

[6] H. Bie, P. Li, F. Chen, and E. Ghaderpour, "An observer-based type-3 fuzzy control for non-holonomic wheeled robots," *Symmetry*, vol. 15, no. 7, p. 1354, Jul. 2023.

[7] H. Cen and B. K. Singh, "Nonholonomic wheeled mobile robot trajectory tracking control based on improved sliding mode variable structure," *Wireless Commun. Mobile Comput.*, vol. 2021, pp. 1–9, Jun. 2021.

[8] F. Chen, X. Qiu, K. A. Alattas, A. Mohammadzadeh, and E. Ghaderpour, "A new fuzzy robust control for linear parameter-varying systems," *Mathematics*, vol. 10, no. 18, p. 3319, Sep. 2022.

[9] X. Chen and X. Zhang, "Global fixed-time stabilization for chained nonholonomic systems via output feedback control," *Int. J. Control, Autom. Syst.*, vol. 21, no. 2, pp. 419–428, Feb. 2023.

[10] A. Emadi, T. Lipniacki, A. Levchenko, and A. Abdi, "A decision making model where the cell exhibits maximum detection probability: Statistical signal detection theory and molecular experimental data," in *Proc. 57th Annu. Conf. Inf. Sci. Syst. (CISS)*, Mar. 2023, pp. 1–4.

[11] A. Emadi, M. Ozen, and A. Abdi, "A hybrid model to study how late long-term potentiation is affected by faulty molecules in an intraneuronal signaling network regulating transcription factor CREB," *Integrative Biol.*, vol. 14, no. 5, pp. 111–125, Aug. 2022.

[12] J. Guo, C. Li, and S. Guo, "A novel step optimal path planning algorithm for the spherical mobile robot based on fuzzy control," *IEEE Access*, vol. 8, pp. 1394–1405, 2020.

[13] Z. Jian, Z. Yan, X. Lei, Z. Lu, B. Lan, X. Wang, and B. Liang, "Dynamic control barrier function-based model predictive control to safety-critical obstacle-avoidance of mobile robot," in *Proc. IEEE Int. Conf. Robot. Autom. (ICRA)*, May 2023, pp. 3679–3685.

[14] B. Kada, A. S. A. Balamesh, K. A. Juhany, and I. M. Al-Qadi, "Distributed cooperative control for nonholonomic wheeled mobile robot systems," *Int. J. Syst. Sci.*, vol. 51, no. 9, pp. 1528–1541, Jul. 2020.

[15] A. Kumar, R. Raj, A. Kumar, and B. Verma, "Design of a novel mixed interval type-2 fuzzy logic controller for 2-DOF robot manipulator with payload," *Eng. Appl. Artif. Intell.*, vol. 123, Aug. 2023, Art. no. 106329.

[16] M. A. L. Khaniki, M. Manthouri, and M. A. Khanesar, "Adaptive non-singular fast terminal sliding mode control and synchronization of a chaotic system via interval type-2 fuzzy inference system with proportionate controller," *Iranian J. Fuzzy Syst.*, vol. 20, no. 6, pp. 171–185, 2023.

[17] J. Li, J. Wang, H. Peng, Y. Hu, and H. Su, "Fuzzy-torque approximation-enhanced sliding mode control for lateral stability of mobile robot," *IEEE Trans. Syst., Man, Cybern., Syst.*, vol. 52, no. 4, pp. 2491–2500, Apr. 2022.

[18] Q. Li, H. Yang, Y. Xia, and H. Zhao, "Switched model predictive control for nonholonomic mobile robots under adaptive dwell time," *IEEE Trans. Cybern.*, early access, Mar. 29, 2023, doi: 10.1109/TCYB.2023.3258667.

[19] Y. Li, S. Dong, and K. Li, "Fuzzy adaptive finite-time event-triggered control of time-varying formation for nonholonomic multirobot systems," *IEEE Trans. Intell. Vehicles*, early access, Aug. 10, 2023, doi: 10.1109/TIV.2023.3304064.

[20] T. Ma, Z. Li, J. Liu, A. F. Alkhateeb, and H. Jahanshahi, "A novel self-learning fuzzy predictive control method for the cement mill: Simulation and experimental validation," *Eng. Appl. Artif. Intell.*, vol. 120, Apr. 2023, Art. no. 105868.

[21] T. A. Mai, T. S. Dang, H. C. Ta, and S. P. Ho, "Comprehensive optimal fuzzy control for a two-wheeled balancing mobile robot," *J. Ambient Intell. Humanized Comput.*, vol. 14, no. 7, pp. 9451–9467, Jul. 2023.

[22] P. Melin and O. Castillo, "An interval type-3 fuzzy–fractal approach for plant monitoring," *Axioms*, vol. 12, no. 8, p. 741, Jul. 2023.

[23] A. Mohammadzadeh, H. Taghavifar, C. Zhang, K. A. Alattas, J. Liu, and M. T. Vu, "A non-linear fractional-order type-3 fuzzy control for enhanced path-tracking performance of autonomous cars," *IET Control Theory Appl.*, vol. 18, no. 1, pp. 40–54, Jan. 2024, doi: 10.1049/cth2.12538.

[24] M. Ou, H. Sun, Z. Zhang, and S. Gu, "Fixed-time trajectory tracking control for nonholonomic mobile robot based on visual servoing," *Nonlinear Dyn.*, vol. 108, no. 1, pp. 251–263, Mar. 2022.

[25] C. Peraza, O. Castillo, P. Melin, J. R. Castro, J. H. Yoon, and Z. W. Geem, "A type-3 fuzzy parameter adjustment in harmony search for the parameterization of fuzzy controllers," *Int. J. Fuzzy Syst.*, vol. 25, no. 6, pp. 2281–2294, Sep. 2023.

[26] S. Poulik and G. Ghorai, "Determination of journeys order based on graph's Wiener absolute index with bipolar fuzzy information," *Inf. Sci.*, vol. 545, pp. 608–619, Feb. 2021.

[27] S. Poulik and G. Ghorai, "Estimation of most effected cycles and busiest network route based on complexity function of graph in fuzzy environment," *Artif. Intell. Rev.*, vol. 55, no. 6, pp. 4557–4574, Aug. 2022.

[28] S. Poulik, G. Ghorai, and Q. Xin, "Explication of crossroads order based on Randic index of graph with fuzzy information," *Soft Comput.*, early access, Dec. 13, 2023, doi: 10.1007/s00500-023-09453-6.

[29] M. J. Rabbani and A. Y. Memon, "Trajectory tracking and stabilization of nonholonomic wheeled mobile robot using recursive integral backstepping control," *Electronics*, vol. 10, no. 16, p. 1992, Aug. 2021.

[30] A. Tarafdar, P. Majumder, M. Deb, and U. K. Bera, "Application of a q-rung orthopair hesitant fuzzy aggregated type-3 fuzzy logic in the characterization of performance-emission profile of a single cylinder CI-engine operating with hydrogen in dual fuel mode," *Energy*, vol. 269, Apr. 2023, Art. no. 126751.

[31] M.-W. Tian, K. A. Alattas, W. Guo, H. Taghavifar, A. Mohammadzadeh, W. Zhang, and C. Zhang, "A strong secure path planning/following system based on type-3 fuzzy control, multi-switching chaotic systems, and random switching topology," *Complex Intell. Syst.*, early access, Oct. 19, 2023, doi: 10.1007/s40747-023-01248-4.

[32] J. Wang, M. T. H. Fader, and J. A. Marshall, "Learning-based model predictive control for improved mobile robot path following using Gaussian processes and feedback linearization," *J. Field Robot.*, vol. 40, no. 5, pp. 1014–1033, Aug. 2023.

[33] L. Wu, H. Huang, M. Wang, K. A. Alattas, A. Mohammadzadeh, and E. Ghaderpour, "Optimal control of non-holonomic robotic systems based on type-3 fuzzy model," *IEEE Access*, vol. 11, pp. 124430–124440, 2023.
[34] Y. Wu and Y. Wang, "Asymptotic tracking control of uncertain non-holonomic wheeled mobile robot with actuator saturation and external disturbances," *Neural Comput. Appl.*, vol. 32, no. 12, pp. 8735–8745, Jun. 2020.
[35] N. Zijie, L. Qiang, C. Yonjie, and S. Zhijun, "Fuzzy control strategy for course correction of omnidirectional mobile robot," *Int. J. Control, Autom. Syst.*, vol. 17, no. 9, pp. 2354–2364, Sep. 2019.

WENKUI XUE received the Graduate degree from the Henan University of Technology. Currently, he is an Associate Professor with the Changzhou Vocational Institute of Mechatronic Technology. His research interests include industrial robot technology and system design research.

BAOZHI ZHOU received the Graduate degree from the Nanjing University of Aeronautics and Astronautics. Currently, he is an Experimental Engineer with the Changzhou Vocational Institute of Mechatronic Technology. His research interests include mechanical engineering and automation.

FENGHUA CHEN received the Graduate degree from the Zhejiang University of Technology. She is currently an Associate Professor with the Zhejiang Guangsha Vocational and Technical University of Construction. Her research interest includes robot control.

HAMID TAGHAVIFAR (Member, IEEE) received the Ph.D. degree from Urmia University, Iran, in 2016. His thesis was primarily on leveraging nonlinear dynamics and data-driven controls to analyze and control complex dynamical systems, such as autonomous vehicles and mobile ground robotics. He was awarded the Horizon Post-doctoral Fellowship from Concordia University, Canada, in 2017. Following that, he joined the Fiat Chrysler Research and Development Center, Windsor, ON, USA, where he worked, until 2019, on industry projects mainly around mechatronics and controls in automated driving. He is currently an Assistant Professor with Concordia University. He has been with Coventry University and IFTC Research Center ever since, pursuing his research activities, teaching, and supervising graduate students on industry-funded projects.

ARDASHIR MOHAMMADZADEH received the B.Sc. degree from the Sahand University of Technology, Tabriz, Iran, in July 2011, the M.Sc. degree from the K.N. Toosi University of Technology, Tehran, Iran, in September 2013, and the Ph.D. degree from the University of Tabriz, Tabriz, in November 2016. In December 2017, he joined the University of Bonab, Bonab, Iran, as an Assistant Professor. He joined the Shenyang University of Technology as a Professor, in September 2022. He is an academic editor and a reviewer of many journals. His research interests include control theory, fuzzy logic systems, machine learning, neural networks, intelligent control, electric vehicles, power systems control, chaotic systems, and medical systems.

EBRAHIM GHADERPOUR received the Ph.D. degree in theoretical and computational science and the Ph.D. degree in remote sensing in Canada, in 2013 and 2018, respectively. He is currently an Assistant Professor with the Department of Earth Sciences, Sapienza University of Rome, Italy. He is also the CEO of Earth and Space Inc., Calgary, Canada. He is an academic editor and a reviewer of many journals. His research interests include big data analytics and artificial intelligence with their applications in remote sensing, geology, geosciences, robotics, and medicine.

Open Access funding provided by 'Università degli Studi di Roma "La Sapienza" 2' within the CRUI CARE Agreement